

# Investigating the Roles of CwID and GerS in *Clostridioides difficile* Spore Cortex Modification

Shaeri Nawar

Thesis submitted to the faculty of the Virginia Polytechnic Institute and State  
University in partial fulfillment of the requirements for the degree of  
Master of Science  
in  
Biological Science

David L. Popham, Chair

Ann M. Stevens

Clayton C. Caswell

Stephen B. Melville

12th May 2025

Blacksburg, VA

Keywords: *Clostridioides difficile*, spores, cortex, peptidoglycan, CwID, GerS,  
sporulation, germination, *Bacillus subtilis*

# Investigating the Roles of CwID and GerS in *Clostridioides difficile* Spore Cortex Modification

Shaeri Nawar

## Academic abstract

*Clostridioides difficile* is a notable nosocomial pathogen distinguished by its capacity to produce spores, essential for its survival and dissemination. The spore cortex, consisting of a modified peptidoglycan layer, is essential for dormancy and germination. This work examines the enzyme CwID, which facilitates the transformation of N-acetylmuramic acid (NAM) into muramic- $\delta$ -lactam (MAL)—a change crucial for adequate cortex production and germination. The lipoprotein GerS is essential for CwID function in *C. difficile*; however, no GerS homolog is present in *Bacillus subtilis*, a well-established model for spore biology. To assess the species requirements for CwID and GerS, we expressed FLAG-tagged versions of *C. difficile* CwID, both in the presence and absence of GerS, in a *B. subtilis*  $\Delta cwid$  background. Despite the effective assembly and integration of all genetic constructs, no expression of FLAG-tagged protein was seen. The data indicates that factors such as translational inefficiency or protein degradation may impede the expression of these heterologous proteins in *B. subtilis*. This contrasts with prior research demonstrating observable production of variants even though they remained non-functional in *B. subtilis*. These findings highlight the significance of the native cellular environment for the functional expression of CwID–GerS and enhance the comprehension of species-specific regulatory mechanisms in spore life. These results may guide future therapy strategies aimed at targeting *C. difficile* germination by inhibiting CwID–GerS-mediated MAL production. This would impede spore germination, presenting a potential approach to avoid infection initiation and diminish recurrence by maintaining remaining spores in a dormant state.

# **Investigating the Roles of CwID and GerS in *Clostridioides difficile* Spore Cortex Modification**

**Shaeri Nawar**

## **Abstract for General Audience**

*Clostridioides difficile* is a bacterium that is dangerous and is known to cause severe intestinal infections, particularly in individuals who are taking antibiotics or residing in hospitals. This bacterium's capacity to generate resistant latent spores that can endure severe conditions and induce recurrent infections is what renders it particularly challenging to eradicate. Two proteins, CwID and GerS, collaborate to produce a unique molecule in the spore cell wall structure known as muramic- $\delta$ -lactam (MAL) in *C. difficile*. MAL is essential for the correct development of spores, which subsequently "wake up" (germinate) and produce infection. We attempted to produce these proteins in *Bacillus subtilis*, a closely related and extensively studied bacterium, to better understand their functionality. Although the genes were successfully inserted, we discovered that the proteins were either not produced or were not functioning normally. This implies that *C. difficile* may necessitate specific cellular factors that are not present in *B. subtilis* to sustain these proteins. By comprehending the mechanisms of these proteins, we can identify novel methods for preventing the germination of *C. difficile* spores. In the future, the prevention of this process could result in more effective treatments that prevent infection or its recurrence.

## **Acknowledgements**

I would like to sincerely thank Dr. David L. Popham, my advisor and committee chair, for his guidance, encouragement, and thoughtful feedback throughout this project. His mentorship has been central to both the completion of this thesis and my growth as a scientist.

I am also grateful to my committee members, Dr. Ann M. Stevens, Dr. Clayton C. Caswell, and Dr. Stephen B. Melville, for their valuable input and support throughout this process.

Many thanks to my lab mates, especially Shreya Choudhary, Safoura Salar, and Marcel Shams Eddin, for their help, discussions, and everyday support in the lab. I would also like to thank Brian J. Kohler for his early mentorship, which helped me find my footing when I joined the lab.

Finally, I am deeply thankful to my family. Thanks to my mom and dad, and my uncles Tuhin and Saiful, for your constant love, support, sacrifices, and belief in me. Sheru, Ghublu, Sib, Sam, Jum, Rehan, Moon, Mim, Fariba, Adri, Piu, your encouragement and presence, near or far, have meant the world to me.

# Table of Contents

CHAPTER 1: INTRODUCTION.....	1
1.1 <i>Clostridioides difficile</i> .....	1
1.2 Overview of <i>C. difficile</i> Infection (CDI).....	1
1.3. Treatment.....	2
1.4. The Life Cycle of Spore-Forming Bacteria.....	2
1.5. Sporulation.....	4
1.6 Structure of spores and mechanisms of resistance.....	5
1.7. Vegetative Peptidoglycan and Cell Wall Integrity.....	8
1.8. Modification of the cortex peptidoglycan.....	9
1.9. Germination in <i>B. subtilis</i> and <i>C. difficile</i> .....	10
1.10. Conversion to Vegetative Cells and Production of <i>C. difficile</i> Toxins.....	10
1.11. Amidases and Their Function in Sporulation.....	11
1.12. Previous studies on amidases in <i>C. difficile</i> .....	12
1.13. Comparative analysis: CwID:GerS in <i>C. difficile</i> against <i>B. subtilis</i> .....	13
1.14. Previous work in the Popham Lab.....	14
1.15. Research Gap and Specific Objectives.....	15
CHAPTER 2: METHODS.....	16
2.1 Construction of Plasmids.....	16
2.2. Validation of Plasmids via Restriction Digestion and Gel Electrophoresis.....	17
2.3. Gibson Assembly of Constructs.....	19
2.4. Transformation of <i>E. coli</i> and Evaluation of Recombinant Plasmids:.....	19
2.5. Preparation of <i>B. subtilis</i> strains.....	20
2.6. Sporulation Conditions.....	20
2.7. Identification of FLAG-Tagged Proteins by Western Blot.....	21
2.8. Evaluation of Spore Germination Efficiency (CFU-Based Assay).....	21
2.9 Extraction of Cortex Peptidoglycan and HPLC Evaluation.....	22
CHAPTER 3: RESULTS.....	23
3.1. Plasmid Isolation and Confirmation:.....	23
3.2. Expression plasmid design and assembly.....	27
3.3. Growth, Sporulation, and Protein Detection using FLAG-Tagged Constructs:.....	37
3.4. Germination efficiency of recombinant <i>B. subtilis</i> strains.....	40
3.5. Spore cortex structure of recombinant <i>B. subtilis</i> strains:.....	42

<b>CHAPTER 4: DISCUSSION .....</b>	<b>44</b>
<b>CHAPTER 5: CONCLUSION.....</b>	<b>47</b>
<b>Reference .....</b>	<b>48</b>

## **CHAPTER 1: INTRODUCTION**

### **1.1 *Clostridioides difficile***

*Clostridioides difficile* is a spore-forming Gram-positive bacterium that is well-known for its involvement in gastrointestinal (GI) infections. The organism is found in two different forms: dormant endospores and metabolically active vegetative cells (1). The GI tract of the host is colonized by the vegetative cells, which can replicate there under favorable circumstances. The vegetative cells are susceptible to external stresses in the GI tract. However, *C. difficile* can produce extremely resistant endospores to guarantee survival and aid in transmission between hosts (2). The significance of *C. difficile* as a persistent pathogen and a major contributor to intestinal illnesses is highlighted by its spores' extensive distribution in both natural and clinical settings. By producing toxigenic strains, *C. difficile* causes symptoms that range from mild diarrhea to fatal colitis by producing toxins that damage the intestinal tract (3).

### **1.2 Overview of *C. difficile* Infection (CDI)**

One of the main causes of infections linked to healthcare worldwide and a serious public health concern is *C. difficile* infection (CDI). The primary manifestation of CDI is antibiotic-associated diarrhea (4). Various GI symptoms are seen, including nausea, fever, diarrhea, and abdominal pain. In extreme situations, it may result in pseudomembranous colitis, a disorder marked by inflammation of the mucosal lining of the colon. Recurrent infections are also common and can cause chronic, incapacitating symptoms. The main risk factors of CDI include antibiotic usage, extended hospital stays, advanced age, and immunosuppression (5). The transmission of *C. difficile* is through the fecal-oral pathway, and the infectious form is its extremely resistant spores. Spores germinate into a vegetative, toxin-producing state in the GI tract after being consumed and

exposed to suitable conditions. This change results in toxin release, harming the intestinal mucosa, and resulting in CDI symptoms. Spores germinate into a vegetative, toxin-producing state in the GI tract after being consumed and exposed to suitable conditions. This change results in toxin release, harming the intestinal mucosa and resulting in CDI symptoms (6).

### **1.3. Treatment**

With an emphasis on efficient medicines and recurrence prevention techniques, CDI care has first-line therapies such as vancomycin and fidaxomicin. While fidaxomicin provides a more focused strategy with a smaller spectrum, reducing damage to the GI flora, vancomycin, when taken orally, works directly in the GI tract. However, therapy is made more difficult by the growing number of *C. difficile* strains that are resistant to drugs. Adjunctive treatments such as fecal microbiota transplantation (FMT) or newly developed toxin-binding medicines may be taken into consideration in cases that are recurring. Preventive measures, such as strict infection control and antimicrobial stewardship, are still essential (7).

### **1.4. The Life Cycle of Spore-Forming Bacteria**

To understand the true mechanism of *C. difficile* infection, shedding light on its life cycle is essential. This life cycle supports its capacity to spread infection and endure in a variety of settings and must be examined more closely to comprehend its transmission and effects. It is important to note that some other spore-forming bacteria, like *B. subtilis*, also undergo the same life cycle as *C. difficile*. This spore-forming bacterial life cycle is a complicated process that includes changes between latent and active phases, which are essential to the pathogen's ability to survive, colonize, and spread. Together, the processes of sporulation, germination, vegetative growth, and toxin synthesis allow the bacteria to survive and spread infection in a variety of settings (8).

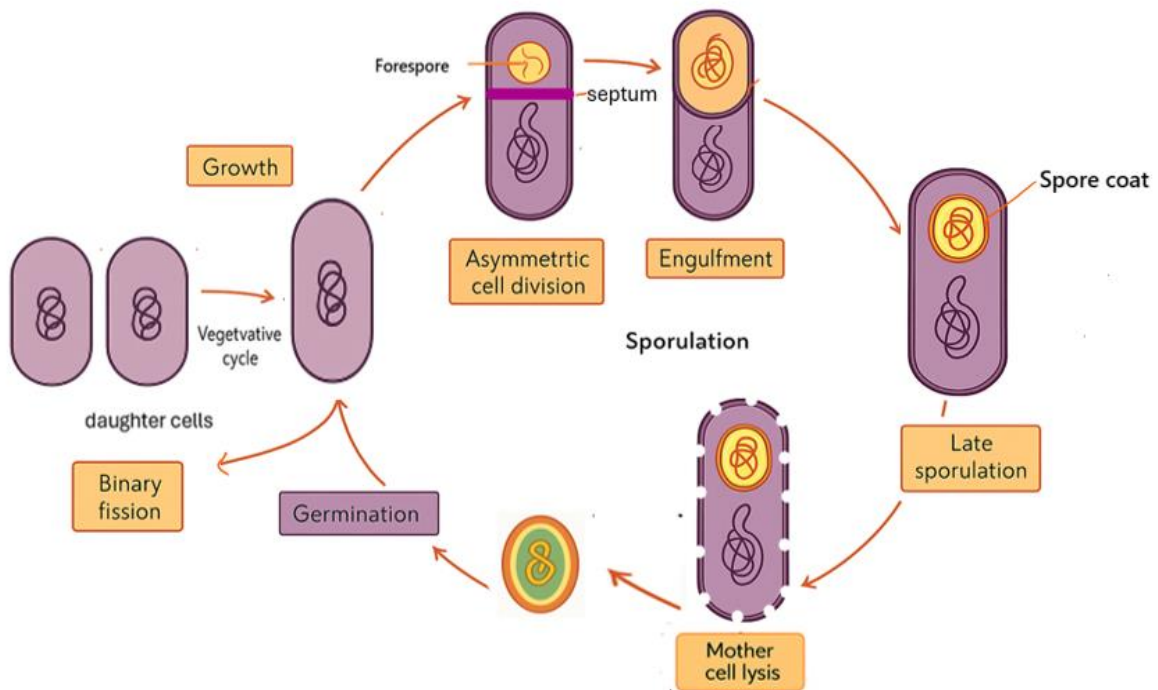


**Figure 1.1: Life cycle of spore-forming bacteria.**

Spore-forming bacteria transition from vegetative cells to dormant spores via sporulation and back to active vegetative cells through germination. The key stages of the life cycle of a spore-forming bacterium include asymmetric cell division, engulfment, spore coat formation, mother cell lysis, and spore germination.

## 1.5. Sporulation

Sporulation is a step-by-step process done by spore-forming bacteria like *B. subtilis* and *C. difficile* to change from the vegetative stage to the sporulating stage. The spores are dormant and extremely heat resistant. This spore formation process results from stress caused by environmental stimuli, quorum sensing, nutritional scarcity, and other detrimental situations (9). Sporulation in all endospore-forming bacteria is regulated genetically by phosphorylating a master regulator called Spo0A. The sigma factors  $\sigma_E$ ,  $\sigma_F$ ,  $\sigma_G$ ,  $\sigma_H$ , and  $\sigma_K$  are successively activated to alter gene expression as the sporulation process progresses (10).

There are four main developmental stages of this process in both *B. subtilis* and *C. difficile*:

1. Asymmetric division: Environmental signals cause the bacterial cell to undergo division into two disparate segments, the larger mother cell (MC) and the smaller forespore (FS). Before this, the chromosome undergoes replication. One copy remains in the mother cell while one copy is allocated to the forespore. This activates cell-type-specific sigma factors— $\sigma_F$  in the forespore and  $\sigma_E$  in the mother cell, which coordinate gene expression to stimulate membrane migration and curvature around the forespore, setting off this process (11).
2. Engulfment: The forespore is the smaller compartment, which is engulfed by the mother cell in a phagocytic fashion, enclosing it within its cytoplasm (12). The double membrane formed by the mother cell enveloping the forespore separates into the internal and outside spore membranes. Following engulfment,  $\sigma_G$  is activated in the forespore, and  $\sigma_K$  becomes active in the mother cell.
3. Maturation: During maturation, supplementary peptidoglycan is polymerized between the inner and outer spore membranes, resulting in a thickened cortex. The spore coat layers are constructed around the external spore membrane. Calcium dipicolinic acid (Ca-DPA), a chelated combination of  $\text{Ca}^{2+}$  and dipicolinic acid, accumulates in the forespore and displaces a significant portion of the

water content. This dehydration enhances spore dormancy and resilience, while augmenting phase brightness under a phase-contrast microscope.

4. Liberation of the Mature Spore: A tightly controlled process driven by  $\sigma_K$  allows the mature spore to be liberated from its parent (mother cell) (8). The resilient architecture released is called the endospore. It consists of a dense core, a spore cortex, a protein shell, and occasionally an exosporium, which ensures its endurance in extreme environments (9).

## **1.6 Structure of spores and mechanisms of resistance**

Bacterial spores produced by *Bacillus*, *Clostridioides*, and analogous species are metabolically inactive under conditions that limit growth. Spores possess several structural layers that enhance their resistance properties with remarkable resilience to ultraviolet radiation, antibiotics, toxic substances, and elevated temperatures. This phenomenon enables their survival in the environment for years without the need for nutrients. Upon the establishment of favorable circumstances, spores germinate and reinitiate the vegetative cycle. The most important feature of an endospore is that it consists of several protective layers surrounding a core (Figure 1.3).

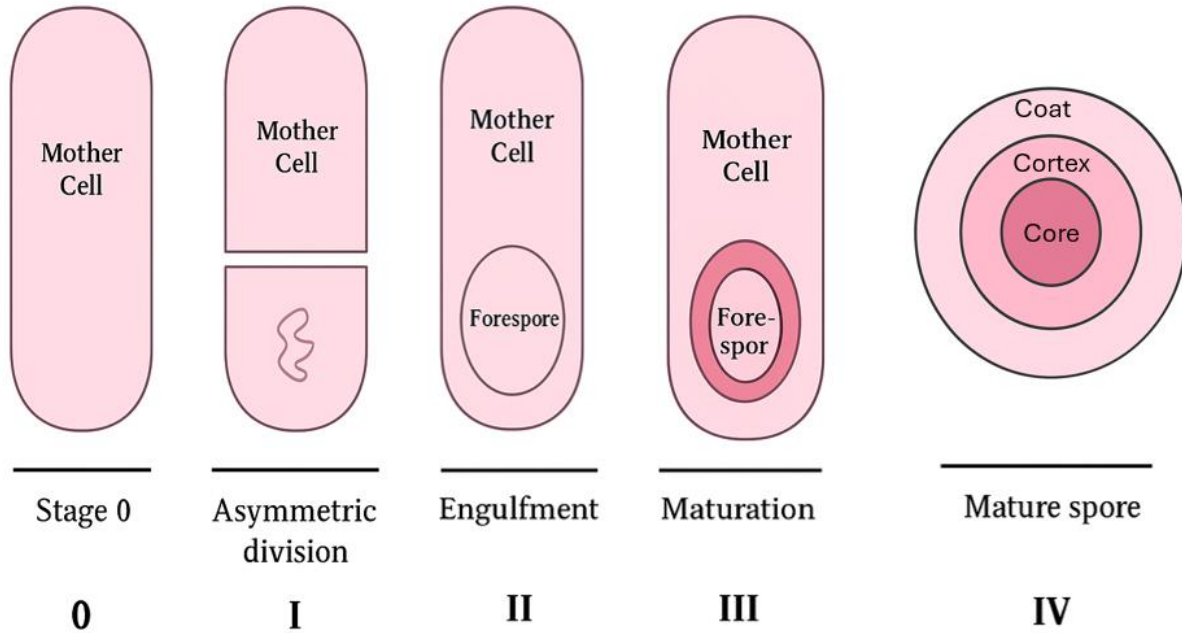


**Figure 1.2: Stages of Sporulation.**

The figure illustrates the main stages of sporulation and the anatomy of the spore in *C. difficile*. While certain strains of *C. difficile* possess the exosporium, others do not. The exosporium structure was excluded from this figure.

The layers, starting from the innermost, are the inner membrane, germ cell wall, cortex, outer membrane, proteinaceous coat, and, in certain species, an exosporium (13). The endospore's core comprises the chromosome, ribosomes, and enzymes, all contained inside a desiccated environment. The spore's resilience is ascribed to its significantly low water content—generally 25–40% of the core's wet weight, in contrast to approximately 80% in vegetative cells—coupled with elevated concentrations of calcium-dipicolinic acid (Ca-DPA) and DNA saturation with  $\alpha/\beta$ -type small acid-soluble proteins (SASPs), which safeguard nucleic acids from harm. SASPs safeguard DNA from UV exposure, whereas Ca-DPA and dehydration impart thermal resistance

(14). The inner membrane of the spore is a densely organized, phospholipid-based structure that exhibits extremely low permeability, significantly restricting—but not completely preventing—the transit of small molecules such as water. This safeguards the spore's genetic material from chemical degradation. The inner membrane also contains germinant receptors that sense environmental cues to trigger germination. During germination, this membrane undergoes structural expansion without new membrane synthesis to accommodate the core's rehydration and metabolic activation (15). The germ cell wall of the spore encases the inner membrane. It consists of unaltered peptidoglycan layers, which subsequently transform into the vegetative cell wall post-germination. This structure inhibits osmotic lysis during cell rehydration. It structurally mimics vegetative peptidoglycan, with alternating N-acetyl glucosamine (NAG) and N-acetylmuramic acid (NAM) with peptide side chains (commonly L-Ala-D-Glu-M-Dpm-D-Ala) (16). The germ cell wall is encased by a robust cortex layer comprised of modified peptidoglycan, which experiences specific modifications. The major alteration is that about 50% of NAM residues are devoid of a peptide side chain and are transformed into muramic- $\delta$ -lactam (MAL), an essential structural feature that aids in cortical disintegration during germination by acting as a recognition factor for germination-specific lytic enzymes (GSLEs) (17-19). The cortex preserves dormancy while facilitating regulated breakdown during germination. The spore coats are the external proteinaceous layers, which offer mechanical protection and resistance to enzymatic degradation and chemical damage (20). These structural elements augment the spore's resilience and durability, ensuring survival in harsh environmental circumstances and significantly contributing to the transmission and recurrence of illnesses caused by spore-forming bacteria.

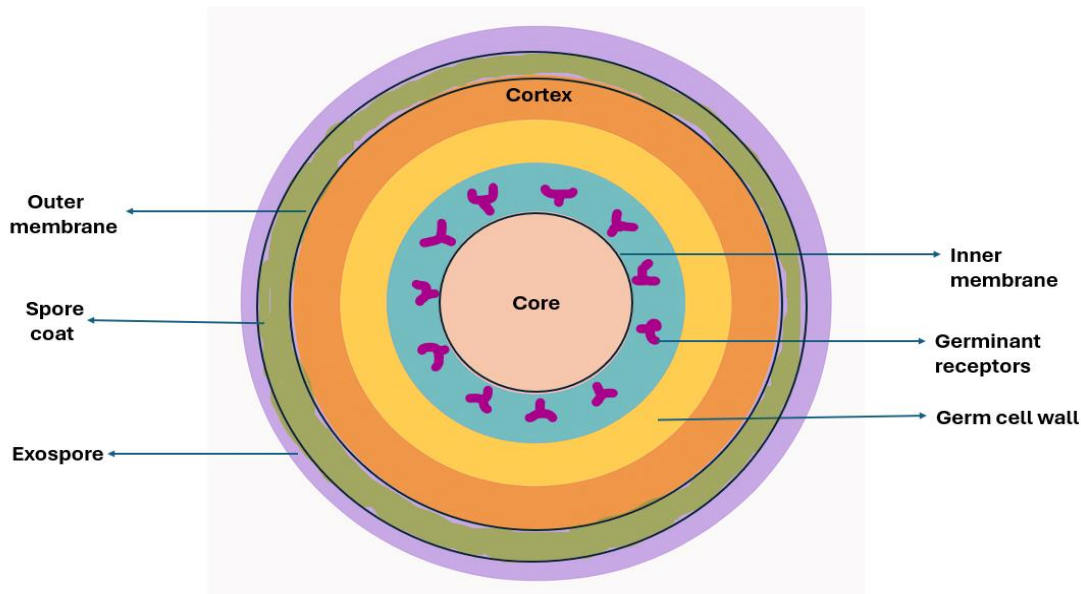


**Figure 1.3: General Schematic diagram of a bacterial spore.**

The figure illustrates different parts of a bacterial spore, which include the exosporium, spore coat, outer membrane, cortex, germ cell wall, inner membrane, with the germinant receptors, and the core.

### **1.7. Vegetative Peptidoglycan and Cell Wall Integrity**

The vegetative cell wall consists of peptidoglycan. This structure offers mechanical stability, osmotic resistance, and preservation of cell morphology (21, 22). The vegetative peptidoglycan layer has alternating N-acetylglucosamine and N-acetylmuramic acid residues, creating glycan strands interconnected by short peptide chains. This ensures structural integrity and resistance to osmotic pressure. Cross-linking peptidoglycan is crucial for maintaining bacterial morphology (23).

## 1.8. Modification of the cortex peptidoglycan

During spore germination, several spore components experience breakdown or recycling. The initial crucial degradative event is the depolymerization of the spore cortex peptidoglycan (PG), which is vital for the thorough hydration of the spore core and the restart of cellular metabolism (24). The spore cortex is a robust layer of altered peptidoglycan, structurally different from the vegetative cell wall, essential for preserving spore dormancy and environmental resilience. A distinctive characteristic is the transformation of approximately 50% of NAM residues into muramic- $\delta$ -lactam (MAL) (8, 25). This alteration renders the cortex vulnerable to germination-specific lytic enzymes (GSLEs), including SleC in *C. difficile* and SleB/CwlJ in *Bacillus* species. The GSLEs identify MAL residues and commence cortex breakdown (16, 26). The cortex is produced between the forespore membranes during sporulation, where it is essential for preserving spore dehydration and enhancing resistance to heat and environmental factors (16, 27). Synthesized during sporulation, GSLEs stay inactive within the latent spore until triggered by germination(28, 29). The controlled disintegration of the cortex facilitates spore core rehydration and metabolic reactivation while maintaining the integrity of the germ cell wall, which subsequently transforms into the vegetative cell wall. The cortex's minimal cross-linking facilitates flexibility, allowing for hibernation while promoting effective germination and vegetative growth.

As GSLEs hydrolyze the cortex, the germ cell wall stays unscathed and eventually transforms into the vegetative cell wall. This structural transformation facilitates a seamless transition from hibernation to active growth (30). Comprehending these anatomical distinctions between cortex and vegetative PG is essential for clarifying how *C. difficile* and *B. subtilis* govern their life cycles and endurance in diverse conditions.

## **1.9. Germination in *B. subtilis* and *C. difficile***

The spore germination processes in *B. subtilis* and *C. difficile* utilize different molecular pathways for the onset and advancement of germination (31). Spore germination in *B. subtilis* is facilitated by germinant receptors (Ger proteins) that identify amino acids such as L-alanine or L-valine, or a mixture of L-asparagine, D-glucose, D-fructose, and potassium ions (AGFK) (21). These germinants are frequently located in decomposing organic material, from which amino acids are liberated by protein breakdown; soil ecosystems, abundant in plant exudates of sugars and amino acids; and host gastrointestinal tracts, wherein nutrients facilitate germinant availability. In contrast to *B. subtilis*, *C. difficile* does not possess canonical germinant receptors and instead utilizes CspC, a pseudoprotease that binds bile acids, specifically taurocholate and cholate (32). Bile acids, present solely in the mammalian small intestine, facilitate the germination of *C. difficile* spores exclusively within the host, hence enhancing its pathogenicity (22, 33). An essential early event in bacterial spore germination is the liberation of calcium-dipicolinic acid (Ca-DPA), a primary component of the spore core. This process is crucial for core hydration, enzyme activation, and metabolic rejuvenation (21).

The release of Ca-DPA coincides with the start of the destruction of the spore cortex. Cortex hydrolysis facilitates further water absorption, reinstating metabolic function and resulting in complete expansion.

## **1.10. Conversion to Vegetative Cells and Production of *C. difficile* Toxins**

The germination process is essential for initiating vegetative cell proliferation and colonizing the digestive system. At this juncture, the cells initiate the manufacture of toxins (8). TcdA and TcdB are the primary toxins generated by toxigenic *C. difficile*. These toxins impair the intestinal epithelial barrier, resulting in inflammation, diarrhea, and, in severe cases, pseudomembranous

colitis. The production of toxins is rigorously regulated and often influenced by dietary and environmental cues (34). Upon effective colonization of the intestine by *C. difficile*, the vegetative cells commence the secretion of virulent factors TcdA and TcdB. The toxin proteins are internalized by intestinal epithelial cells, disrupting the Rho-family of GTPases, hence interfering with the host cell cycle, actin modification, and cytokine production. This will ultimately result in the demise of the host cell (35). TcdA and TcdB enhance the bacterium's adhesion to the epithelium and cause harm to the epithelial cells. This results in the recruitment of neutrophils, leading to inflammation and diarrhea. Should the infection persist, the epithelium will commence degradation due to necrosis, resulting in lesions and ultimately pseudomembranous plaques (36).

### **1.11. Amidases and Their Function in Sporulation**

Amidases are a category of peptidoglycan hydrolases that sever the peptide side chains from N-acetylmuramic acid (NAM) residues in glycan strands. These enzymes are ubiquitous, present in several bacterial species, and have also been identified in insects and humans as peptidoglycan recognition proteins (PGRPs) (37). Their role is essential in processes like bacterial cell division, where they hydrolyze crosslinked peptidoglycan layers to facilitate the separation of daughter cells, exemplified by AmiC in *Escherichia coli*. Nonetheless, due to the capacity of peptidoglycan hydrolases, such as amidases, to dismantle bacterial cell walls, their activity necessitates stringent regulation. For example, in *Staphylococcus aureus*, amidase activity is regulated through interaction with regulatory proteins, inhibiting unregulated breakdown (38). In *B. subtilis* sporulation, the amidase CwID is crucial for altering the spore cortex peptidoglycan. CwID cleaves the peptide side chains from NAM residues, enabling further deacetylation by PdaA, which transforms NAM into muramic- $\delta$ -lactam (MAL) (Figure 1.4).

This alteration is essential as it facilitates the selective degradation of the spore cortex during germination while preserving the structural integrity and dormancy of the spore (39).

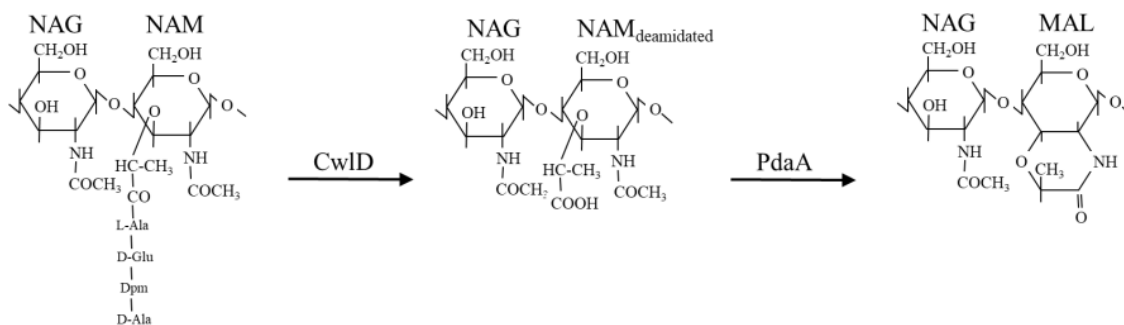


**Figure 1.4: Cortex peptidoglycan modification in spore-forming bacteria (*B. subtilis*).**

The figure illustrates the formation of muramic- $\delta$ -lactam (MAL) to produce cortex peptidoglycan in spore-forming bacteria. The production of muramic- $\delta$ -lactam is completed when CwID deamidates NAM, removing the peptide side chain, and PdaA deacetylates converting NAM into MAL.

### 1.12. Previous studies on amidases in *C. difficile*

In contrast to *B. subtilis*, where CwID operates autonomously, the activity of CwID in *C. difficile* requires the presence of GerS, a distinctive lipoprotein specific to the Peptostreptococcaceae family (40). GerS is important for stabilizing CwID and facilitating its zinc-binding activity, which is crucial for optimal enzyme function (41). *C. difficile* CwID could not bind zinc without the co-expression of GerS, indicating that GerS functions as a stabilizing agent. The evidence for this involvement is derived from crystallization investigations, which revealed that CwID alone could

not be crystallized, whereas the CwID:GerS complex effectively produced crystal structures, underscoring their interdependent functionality. To elucidate the CwID: GerS interaction, researchers analyzed its structure via X-ray crystallography. The findings indicated that CwID: GerS constitutes a hetero tetramer, comprising a GerS homodimer associated with two distinct CwID monomers. Each GerS molecule engages with a CwID monomer in a symmetrical configuration. These findings reinforce the notion that GerS stabilizes CwID via promoting Zn<sup>2+</sup> binding, as tests demonstrated that the CwID: GerS complex eluted at a higher apparent molecular weight in the presence of Zn<sup>2+</sup> ions. Significantly, the GerS residue Met22 directly binds with Zn<sup>2+</sup>, collaborating with CwID residues to preserve the enzyme's functioning (42).

### **1.13. Comparative analysis: CwID:GerS in *C. difficile* against *B. subtilis***

The sporulation mechanism in *C. difficile* largely mirrors that of *B. subtilis*, with the notable distinction of the necessity of GerS for CwID activation. In *B. subtilis*, CwID operates independently, whereas in *C. difficile*, CwID remains dormant in the absence of GerS. The species-specific reliance on GerS indicates that the *C. difficile* forespore has distinct regulatory mechanisms for cortical remodeling. Insertion of *B. subtilis* *cwID* into a *C. difficile*  $\Delta cwID$  strain did not restore function, demonstrating that GerS is crucial for CwID activity in *C. difficile* (42). Comparative research elucidates structural and functional disparities in the CwID-GerS enzyme complex among bacterial species. *B. subtilis* depends only on CwID and PdaA for cortical modification, where amidase CwID cleaves the peptide side chain from N-acetylmuramic acid (NAM), and PdaA deacetylates NAM, resulting in its transformation into muramic- $\delta$ -lactam (MAL). On the contrary, *C. difficile* exhibits a distinct reliance on GerS, highlighting the evolutionary diversity in spore biological mechanisms (41, 43). As a result, the synthesis of muramic- $\delta$ -lactam (MAL), an essential structural alteration in spore cortex peptidoglycan,

transpires via a two-step enzymatic mechanism. Initially, CwID cleaves the peptide side chain from NAM, followed by PdaA, facilitating the transformation of NAM into MAL through the formation of a lactam ring.

#### **1.14. Previous work in the Popham Lab**

Previous research by Brian Kohler in the Popham lab focused on the function of CwID and GerS in cortex peptidoglycan (PG) modification in *C. difficile*. Kohler's study demonstrated that CwID is necessary for transforming N-acetylmuramic acid (NAM) into muramic- $\delta$ -lactam (MAL), a vital alteration for cortex breakdown during germination. This work was done by muropeptide analysis. Notably, each muropeptide is a repetitive subunit of peptidoglycan, consisting of a disaccharide and a peptide chain. It may originate from both the cortex and vegetative PG.

The degradation of peptidoglycan releases muropeptides. High-performance liquid chromatography (HPLC) studies indicated that muropeptides containing MAL were present in *B. subtilis* wild-type spores but absent in  $\Delta cwID$  mutant spores, thereby affirming the critical function of CwID in MAL synthesis and cortical alteration (44). In *C. difficile*, CwID alone was insufficient for MAL synthesis and necessitated the presence of GerS for functional efficacy.

Kohler tried to complement a *B. subtilis*  $\Delta cwID$  strain with *C. difficile* *cwID* to test whether it might act in a different system. Even when co-expressed with GerS, *C. difficile* *cwID* failed to restore MAL generation. This implies that CwID's role could be species-specific. Further biochemical testing by Kohler showed that GerS increases the Zn<sup>2+</sup> binding affinity of CwID and stabilizes its structure. Kohler then conducted peptidoglycan-binding experiments demonstrating that CwID binds weakly to PG, but its association is much enhanced when complexed with GerS, therefore supporting a function for GerS in enzyme localization or activation. These results reveal important

new perspectives on how *C. difficile* alters its cortical PG and why CwID needs GerS for its operation, therefore providing possible targets for interrupting spore germination(41).

### 1.15. Research Gap and Specific Objectives

- Prior investigations demonstrated that *C. difficile* CwID and GerS could be expressed in *B. subtilis*; nevertheless, they failed to restore functionality. What remains ambiguous is whether *C. difficile* CwID and GerS are expressed at sufficient levels in *B. subtilis*. If the CwID and GerS are sufficiently produced, then are they functional or do they remain non-functional? Do they necessitate *C. difficile*-specific co-factors or regulatory components?
- Objective 1: To evaluate the strength of expression of *C. difficile* *cwID* (individually or in conjunction with *gerS*) in a *B. subtilis*  $\Delta$ *cwID* mutant.
  - Expression will be validated using Western blot analysis.
- Objective 2: To ascertain the ability of *C. difficile* GerS and CwID to complement CwID function in *B. subtilis*.
  - Complementation will be evaluated through spore germination and cortex PG structure analysis.
  - The results will elucidate whether GerS is needed for CwID functionality and if species-specific elements are necessary.

## CHAPTER 2: METHODS

### 2.1 Construction of Plasmids

Plasmids were engineered using the pBS1E vector, a framework suitable for cloning in *Escherichia coli* and chromosomal integration in *B. subtilis*. This vector contains an ampicillin [100 µg/mL] resistance gene for selection in *E. coli*, an erythromycin resistance gene for *B. subtilis*, and a red fluorescent protein (RFP) gene for red/white screening. Constructs were developed for chromosomal integration at the *amyE* locus in *B. subtilis*. The genes utilized in this investigation were sourced from plasmids previously created by Dr. Aimee Shen and some by Brian Kohler (Table 2.1). The combinations comprised *cwID* and *gerS* genes from *Clostridioides difficile*, *cwID* from *B. subtilis*, and *Clostridium perfringens*. Inserts were produced using PCR with gene-specific primers (primers specific to genes for this purpose have been shown in Table 3.1, and the primer sequence and description are given in Table 2.1) that had overlapping areas suitable for Gibson Assembly. Purified PCR products were ligated into the linearized pBS1E vector, which had been digested with *SpeI* and *XbaI*. After transforming *E. coli* VE3 cells using electroporation, white colonies selected on ampicillin [100 µg/mL] plates were tested for the presence of inserts through restriction digestion and subsequently verified by Sanger sequencing. Plasmid DNA underwent additional purification using polyethylene glycol (PEG) precipitation, and its quality was evaluated using Nanodrop spectrophotometry. Only plasmids confirmed by sequencing were utilized for transformation into the *B. subtilis*  $\Delta cwID:KnR$  strains. To verify the accuracy of the gene inserts, plasmids (pDNA) underwent Sanger sequencing using the service at the Fralin Life Sciences Institute. Sequencing was performed utilizing primers (primer number 973+974) (Table 2.1).

## 2.2. Validation of Plasmids via Restriction Digestion and Gel Electrophoresis

To confirm the presence and integrity of the target gene inserts, isolated plasmid DNAs were subjected to restriction digestion followed by agarose gel electrophoresis. Two distinct restriction digestion techniques were employed for insert verification. The preliminary technique (RD-1) employed a single restriction enzyme that cuts outside the insert region and a second enzyme that cleaves within the target gene. This methodology was devised to verify digestion patterns and the presence of the insert. The second procedure (RD-2) utilized two restriction enzymes flanking the gene insert, therefore excising the entire insert and confirming its expected size and detachment from the plasmid backbone. Each plasmid design was subjected to digestion using a specific combination of enzymes appropriate for its respective insert. The expected band patterns from the RD-1 and RD-2 experiments aligned with the predicted sizes for each gene construct, validating the successful cloning of the gene inserts together with their correct orientation and integrity. The digestion patterns collectively verified the precise presence and dimensions of inserts in all plasmid preparations.

To verify the accuracy of the gene inserts, plasmids (pDNA) underwent Sanger sequencing using the service at the Fralin Life Sciences Institute. Sequencing was performed utilizing primers (primer number 973+974) (Table 2.1) that encompass the *cwlD* and *gerS* gene insertion regions to guarantee thorough coverage of the cloned sequences.

The resulting data were analyzed using the software 4peaks, followed by alignment with the expected reference sequences utilizing DNA Star (SeqMan Ultra).

**Table 2.1: Primers used in this study.**

Primer number	Description	Sequence	Primer use
956	BsCwlDp-RBS_fwd	AAGCTTATCGAATTCGCGGCCGCTTCTAGACAGTGTAAGCTTCGCATGCG	PCR amplification of <i>B.subtilis cwlD</i> promoter region
957	BsCwlDp-RBS_rev	ACTTTTTTCTCACCCCTTCCCCTCCCGCTTG	PCR amplification of <i>B.subtilis cwlD</i> promoter region
958	BsCwlDp-RBS_rev	ACTTCTCACCCCTTCCCCTCCCGCTTG	PCR amplification of <i>B.subtilis cwlD</i> promoter region
959	CdGerS_fwd	GGAGGGGAAGGGGTGAGAAAAAGTGGACC	PCR amplification of <i>C. difficile gerS</i> gene
960	CdGerS_rev	AAATCCCTCCTATTAGTTTCTGTATTCAAAATCTTTG	PCR amplification of <i>C. difficile gerS</i> gene
961	CdRBS+CwlD+Term_fwd	ATACAGAAACTAATAGGAGGGATTTGTGAGAAAG	PCR amplification of <i>C.difficile cwlD 3Xflag</i>
962	CdRBS+CwlD+Term_rev	TTTGGCCGACTGCAGCGCCGCTACTAGTATAAAAAATAAGAAGCTGCAAATG	PCR amplification of <i>C.difficile cwlD 3Xflag</i>
964	CdRBS+CwlD+Term_fwd	AGGGGAAGGGGTGAGAAAGTACATAAAACATATAATTTTAG	PCR amplification of <i>C.difficile cwlD 3Xflag</i>
1022	BS RBS R	TTTCTCATCCCTTCCCCTCCCGCTTG	PCR amplification of <i>B.subtilis cwlD</i> promoter region
1023	BS CWLD F	AGGGGAAGGGATGAGGAAAAAGCTTAAATGGC	PCR amplification of <i>B.subtilis cwlD-3xFLAG</i>
1063	BsCwlDp-RBS-CpcwlD_rev	TTTTCTTCATCCCTTCCCCTCCCGCTTG	PCR amplification of <i>B. subtilis cwlD promoter-RBS</i> for expressing <i>C.perfringens cwlD</i>
1064	C.p. CWLD F	AGGGGAAGGGATGAAGAAAATAATGAAAATAGTGTC	PCR amplification of <i>C. perfringens. cwlD-3xFLAG</i>
1065	CdGerS-3xFLAG_rev	AAATCCCTCCTATTATTTGTCATCGTCATCC	PCR amplification of <i>C. difficile gerS-3xFLAG</i>
1066	CdRBS+CwlD+Term_fwd	CGATGACAAATAATAGGAGGGATTTGTGAGAAAG	PCR amplification of <i>C. difficile. cwlD(E199A)</i>
973	pBS1CEKinsert Forseq	GAGTATTCCAAACTGGAC	DNA sequencing of the pBS1 plasmid insert
974	pBS1CEKinsert Revseq	AAGGATTTGAGCGTAGCG	DNA sequencing of pBS1 plasmid insert

The reference sequences were derived from annotated plasmid maps and sequence files previously obtained from Dr. Aimee Shen and Brian Kohler. All plasmids were confirmed to contain precise gene insertion free from mutations, frameshifts, or sequence discrepancies.

### **2.3. Gibson Assembly of Constructs**

Gibson Assembly was employed to attach multiple DNA fragments into a singular plasmid backbone, following the methodology specified by New England Biolabs (2020). This technique facilitated the efficient incorporation of target genes into the linearized pBS1E vector via overlapping homologous sequences.

The assembly designs incorporated the insertion of *cwID* genes, each tagged with a C-terminal 3×FLAG, from *C. difficile*, *B. subtilis*, and *C. perfringens* separately. Additional constructs were linked with *C. difficile gerS* upstream of either the wild-type or FLAG-tagged *cwID*. Additionally, a catalytically inactive *cwID(E199A)* mutant was developed, substituting the glutamate at position 199—essential for zinc coordination in the active site—with alanine, thus rendering the enzyme nonfunctional (42). The E199A mutant functioned as a negative control in functional experiments.

### **2.4. Transformation of *E. coli* and Evaluation of Recombinant Plasmids:**

After Gibson Assembly, recombinant plasmids were delivered into electrocompetent *E. coli* VE3 cells via electroporation. Transformants were selected on LB agar plates containing ampicillin (100 µg/mL), and white colonies, indicative of effective disruption of the vector's red fluorescent protein (RFP) gene, were chosen for further examination.

Plasmid DNA was isolated from overnight cultures of chosen colonies. The presence and integrity of gene inserts were initially evaluated using restriction enzyme digestion. Clones displaying the anticipated digestion patterns were further validated by Sanger sequencing to establish sequence

fidelity and confirm the lack of mutations introduced during PCR amplification or Gibson Assembly.

## **2.5. Preparation of *B. subtilis* strains**

Plasmids were incorporated into a mutant strain of *B. subtilis*  $\Delta cwID::Kn^R$  for recombination at the *amyE* locus. Transformants were selected through culture on 2xSG medium with 50  $\mu\text{g/ml}$  kanamycin, 0.5  $\mu\text{g/ml}$  erythromycin, and 12.5  $\mu\text{g/ml}$  lincomycin. After genomic DNA isolation, PCR was conducted with gene-specific primers (primers specific to genes for this purpose have been shown in Table 3.1, and the primer sequence and description are given in Table 2.1) to amplify the inserted genes for confirmation. The amplified products were subsequently analyzed using Sanger sequencing to verify accurate integration.

## **2.6. Sporulation Conditions**

*B. subtilis* strains containing FLAG-tagged complementation constructs were cultivated in 2xSG medium at 37°C with agitation to facilitate sporulation. Cultures were monitored until an optical density at 600 nm ( $\text{OD}_{600}$ ) of 3.0, designated as  $T_0$ , was attained, signifying the onset of sporulation. To assess protein expression during sporulation, samples were collected four hours post- $T_0$ , referred to as  $T_4$ , a phase associated with mid-to-late sporulation processes, including cortex and spore coat formation. The selection of  $T_0$  and  $T_4$  time points was guided by prior studies demonstrating that notable morphological changes and the production of sporulation-associated proteins occur during these intervals (45).

## **2.7. Identification of FLAG-Tagged Proteins by Western Blot**

At T<sub>4</sub>, samples of culture were harvested using centrifugation (5000 rpm for 5 minutes at 4°C), resuspended in lysis buffer (20 mM Tris-HCl, pH 7.5; 10 mM EDTA; 1 mg/mL lysozyme; 1 mM PMSF; 10 µg/mL DNase I; and 100 µg/mL RNase A), and incubated at 37°C for 10 minutes. Equal volumes of 2X Laemmli sample buffer were added to each lysate and then heated at 80°C for 5 minutes. Protein samples were separated using 12% SDS-PAGE gels (Bio-Rad) and subsequently transferred to PVDF membranes. Stain-Free fluorescence imaging was used to visualize total protein content directly on the membrane, allowing for verification of equal loading and normalization of western blot signals. Immunoblotting was performed using a monoclonal anti-FLAG antibody to detect 3xFLAG-tagged CwID and GerS. A horseradish peroxidase (HRP)-conjugated secondary antibody was utilized for detection, followed by chemiluminescence visualization using the Clarity Max Western ECL substrate (Bio-Rad). Blot signals were acquired and analyzed using Bio-Rad Image Lab 6.1 software. This approach enabled the accurate and sensitive detection of FLAG-tagged proteins across diverse experimental conditions.

## **2.8. Evaluation of Spore Germination Efficiency (CFU-Based Assay)**

The spores were pelleted from the stocks by centrifugation. The supernatant was discarded, and the pellets were resuspended in 25 mL of sterile distilled water. OD<sub>600</sub> was measured using a 1:1000 dilution of the spore suspension, and the concentration was adjusted to ensure that a final suspension at OD<sub>600</sub> = 0.2 in sterile water was achieved. The spore suspension was diluted in sterile water in a series of 10-fold increments (100 µL into 900 µL) until it reached 10<sup>-5</sup>. To calculate the total viable germinable spores, 50 µL aliquots were

deposited onto LB agar plates (without antibiotics) from these dilutions. The dilutions were selected following the strain:

- Wild-type spores were plated at  $10^{-4}$  and  $10^{-5}$  dilutions.
- For the  $\Delta cwID$  mutant spores,  $10^{-1}$ ,  $10^{-2}$ , and  $10^{-3}$  dilutions were plated.
- The *cwID* complementation strains were plated at dilutions ranging from  $10^{-1}$  to  $10^{-4}$ .

The germination efficacy was quantified by counting the number of colony-forming units (CFUs) on the plates, which were incubated overnight at 37°C.

## **2.9 Extraction of Cortex Peptidoglycan and HPLC Evaluation**

Peptidoglycan from the cortex was extracted from freshly purified *B. subtilis* spores. For each strain, approximately 30 OD<sub>600</sub> units of spores were harvested and processed as previously described (41). Peptidoglycan samples were digested with Mutanolysin (Sigma, 125 units) in 250  $\mu$ L of 12.5 mM sodium phosphate buffer (pH 5.5) and incubated overnight at 37°C. Mutanolysin specifically cleaves at the interface of N-acetylmuramic acid (NAM) and N-acetylglucosamine (NAG), while abstaining from cleavage between muramic- $\delta$ -lactam (MAL) and NAG, hence enabling the analysis of MAL-containing fragments. Following digestion, the materials were centrifuged at 15,000  $\times$  g for 15 minutes to remove insoluble debris. The supernatants were collected, freeze-dried, and chemically reduced with sodium borohydride (NaBH<sub>4</sub>) to stabilize the muropeptides. The reduced samples were further examined using reverse-phase High-Performance Liquid Chromatography (HPLC) with a methanol gradient. Elution profiles were recorded at 206 nm, and peak identification was performed by comparing with recognized muropeptide standards and existing literature. Peaks linked to MAL-containing muropeptides were employed to assess amidase activity and suitable cortical maturation.

## CHAPTER 3: RESULTS

### 3.1. Plasmid Isolation and Confirmation:

High-quality plasmid DNA was extracted from all seven bacterial strains (Table 3.1). All preparations had A<sub>260</sub>/A<sub>280</sub> ratios ranging from 1.76 to 1.96, signifying good purity among the samples. Plasmid DNA was obtained in adequate quantity for subsequent applications. All plasmids were validated using restriction digestion (Figure 3.1). The identified banding patterns corresponded with anticipated fragment sizes for both internal cuts (named RD-1 in Table 3.2) and complete insert excisions (named RD-2 in Table 3.2). Minor variations or incomplete digestion were seen in a limited number of samples (e.g., DPVE1023 in RD-1 and DPVE939 in RD-2), whereas most samples yielded distinct and anticipated bands (Table 3.2). The minor variations were deemed negligible, as at least one restriction digestion pattern for all samples (either RD-1 or RD-2) yielded the correct-sized band. The pDNA was also confirmed by performing Sanger sequencing, which validated the existence and precision of all gene insertions. All chromatograms corresponded with the anticipated sequences. As a result, it can be confirmed that all the plasmids were successfully isolated with the correct inserts.

**Table 3.1: Plasmids used.**

Strain	Prepared by	Plasmid	Description	Antibiotic resistance
DPVE 714	Brian Kohler	pBS1E	Cloning vector backbone	Ampicillin
DPVE 937	Brian Kohler	pDPVE 937	<i>Bacillus subtilis</i> <i>cwIDp-RBS-</i> <i>Clostridioides difficile</i> <i>cwID</i>	Ampicillin
DPVE 938	Brian Kohler	pDPVE 938	<i>Bacillus subtilis</i> <i>cwIDp-RBS-</i> <i>Clostridioides difficile</i> <i>gerS-</i> <i>cwID</i>	Ampicillin
DPVE 939	Brian Kohler	pDPVE 939	<i>Bacillus subtilis</i> <i>cwIDp-RBS-</i> <i>Clostridioides difficile</i> <i>gerS-</i> <i>cwID(E199A)</i>	Ampicillin
DPVE 1022	Dr. Aimee Shen	Pmtl-yn1c- CdcwID- 3xFLAG	<i>Clostridioides difficile</i> <i>cwID</i> with <i>C-terminal 3×FLAG</i> under <i>Pmtl</i> <i>promoter</i>	Chloramphenicol
DPVE 1023	Dr. Aimee Shen	Pmtl-yn1c- BsubcwID- 3xFLAG	<i>Bacillus subtilis</i> <i>cwID-3×FLAG</i> under <i>Pmtl</i> promoter	Chloramphenicol
DPVE 1024	Dr. Aimee Shen	Pmtl-yn1c- CperfcwID- 3xFLAG	<i>Clostridium perfringens</i> <i>cwID-</i> <i>3×FLAG</i> under <i>Pmtl</i> promoter	Chloramphenicol

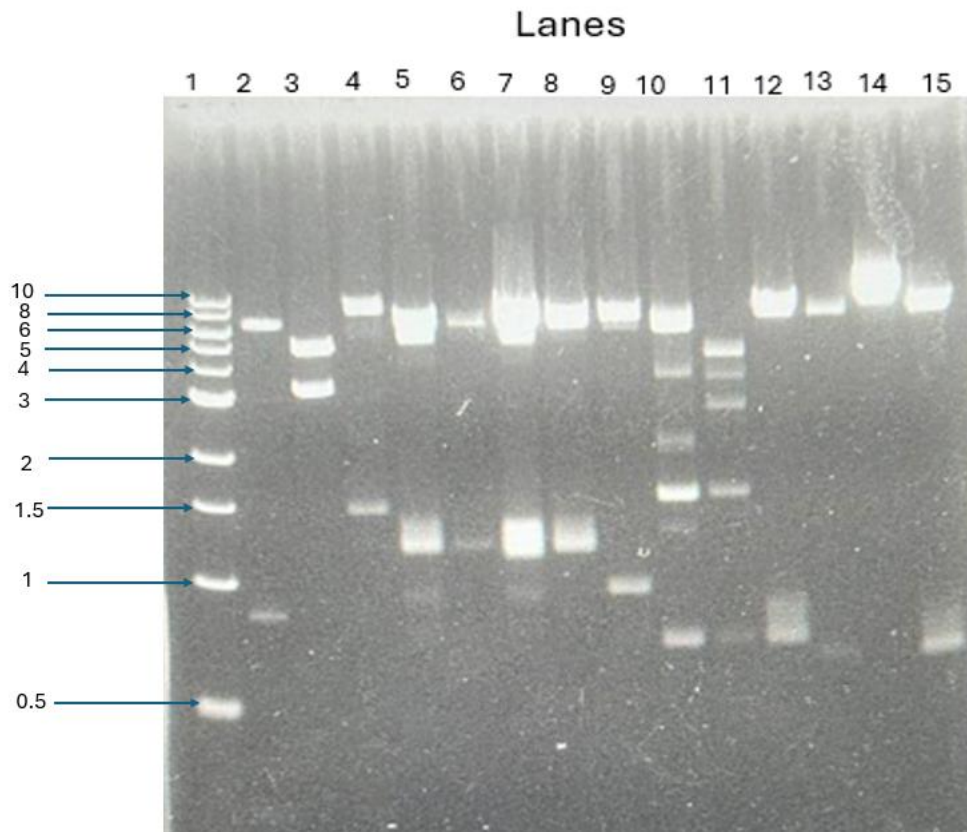


**Figure 3.1: Gel image of restriction-digested pDNA to verify structures.**

All plasmids were validated using restriction digestion. The identified banding patterns corresponded with anticipated fragment sizes for both internal cuts (named RD-1 in table 1.2) and complete insert excisions (named RD-2 in table 1.2).

**Table 3.2 Restriction Digestion verification of plasmid constructs:**

Lane	Sample	Description	Restriction Enzyme(s)	Expected Bands (bp)	Result
1	LADDER	—	—	—	—
2	937 (RD1)	<i>B.s cwlDp-RBS-C.d. cwlD</i>	BamHI + PstI	1043 + 6083	Correct
3	938 (RD1)	<i>B.s cwlDp-RBS-C.d. gerS-cwlD</i>	BamHI + SalI	3065 + 4664	Correct
4	939 (RD1)	<i>B.s cwlDp-RBS-C.d. gerS-cwlD(E199A)</i>	BamHI + PstI	1683 + 6046	Correct
5	1022 (RD1)	<i>CdcwlD-3xFLAG</i>	NotI + PvuII	1173 + 5942	Correct
6	1023 (RD1)	<i>BsubtiliscwlD-3xFLAG</i>	NotI + PvuII	1182 + 5942	Incorrect
7	1024 (RD1)	<i>CperfcwlD-3xFLAG</i>	NotI + PvuII	1140 + 5942	Correct
8	1023 (RD1)	<i>BsubtiliscwlD-3xFLAG</i>	NotI + PvuII	1182 + 5942	Correct
9	937 (RD2)	<i>B.s cwlDp-RBS-C.d. cwlD</i>	BamHI + PvuII	942 + 6184	Correct
10	938 (RD2)	<i>B.s cwlDp-RBS-C.d. gerS-cwlD</i>	BamHI + PvuII	1545 + 6105	Incorrect
11	939 (RD2)	<i>B.s cwlDp-RBS-C.d. gerS-cwlD(E199A)</i>	BamHI + PvuII	1545 + 6105	Incorrect
12	1022 (RD2)	<i>CdcwlD-3xFLAG</i>	NotI + SacI	715 + 6400	Correct
13	1023 (RD2)	<i>BsubtiliscwlD-3xFLAG</i>	NotI + SacI	654 + 6470	Correct
14	1024 (RD2)	<i>CperfcwlD-3xFLAG</i>	NotI + BsmI	875 + 6207	Correct
15	1023 (RD2)	<i>BsubtiliscwlD-3xFLAG</i>	NotI + SacI	654 + 6470	Correct

Note: RD-1 denotes restriction digestion employing two enzymes; one cleaves within the insert while the other cleaves externally, hence verifying the existence of the insert. RD-2 employs two enzymes surrounding the insert to entirely remove it and verify its anticipated size.

### 3.2. Expression plasmid design and assembly

Constructs A–G were designed to express several combinations of *cwlD* and *gerS* genes under control of the *B. subtilis* *cwlD* promoter and RBS, coupled with a 3xFLAG tag for detection (Figure 3.2). Together with *gerS*, from *C. difficile*, *B. subtilis*, and *C. perfringens*, these constructs comprised combinations of wild type, tagged, and catalytically inactive (E199A) forms of *cwlD*. They were designed to enable comparative functional research between many species and expression settings.

PCR products containing each required genetic element were prepared (Table 3.3) and were analyzed by agarose gel electrophoresis (Figure 3.3). Each band corresponded to the anticipated product dimensions, as specified in Table 3.3. No non-specific bands or primer-dimer artifacts were detected, which did not impede subsequent cloning efforts. Included representative amplicons were constructs for the expression of *B. subtilis* *cwlD* (118 bp), *C. difficile* *cwlD*-3xFLAG (1047 bp), *C. perfringens* *cwlD*-3xFLAG (1014 bp), and *C. difficile* *gerS* (615 bp). The data collectively indicate that the PCR technique effectively generated high-quality templates for subsequent molecular modifications.

The plasmid vector pBS1E was linearized by XbaI and SpeI digestion (Figure 3.4). Two separate DNA fragments were found by agarose gel electrophoresis: a smaller ~1.1 kb band for the removed RFP gene and a large ~6 kb band corresponding to the plasmid backbone. Gel extraction followed by purification effectively recovered the bigger fragment and produced high-quality DNA fit for downstream cloning.

The prepared PCR products and the linearized plasmid backbone were used for Gibson Assembly of the desired plasmids (Table 3.4). Gibson-assembled DNA was transformed into *E. coli* and

plated on selective LB + ampicillin agar plates. For Assemblies A through G, white colonies revealed appropriate plasmid integration and RFP disturbance. Assemblies were confirmed first by restriction digestion (Figure 3.5 and Table 3.5). DNA sequencing further validated the accuracy and orientation of all inserts except A. The other sequences matched expected templates with high fidelity, including the point mutation (E199A) in the catalytic site of CwID. No frameshifts or unintended mutations were observed. Assembly A, initially unsuccessful, was attempted again through re-assembly, transformation, and sequencing, but still failed to produce the desired product.

Assemblies B–G were finished and verified by restriction digest and DNA sequencing. All five advanced for *B. subtilis* chromosomal integration and additional study. By contrast, Assembly A (*C. difficile cwID-3xFLAG*) routinely failed at the assembly level. Multiple attempts produced no colonies or colonies that contained incorrect plasmids. The construction could not be retrieved after reevaluating primers and working to solve any potential strain problems. As a result, only the constructs with confirmed insert identification and proper configuration were selected for further downstream investigations.

Successful generation of MLS-resistant *B. subtilis*  $\Delta cwID$  transformants resulted from chromosomal integration of plasmid constructs at the *amyE* locus. Effective double-crossover recombination events were confirmed by PCR amplification with insertion-specific primers. All transformants confirmed construct integration by generating amplicons of the expected sizes. (Figure 3.6 and Table 3.6) With no mutations found in the integrated gene areas, Sanger sequencing of these PCR products verified that the recombined constructions preserved sequence integrity. Stored and ready for downstream phenotypic study and protein expression research were the validated *B. subtilis* strains.

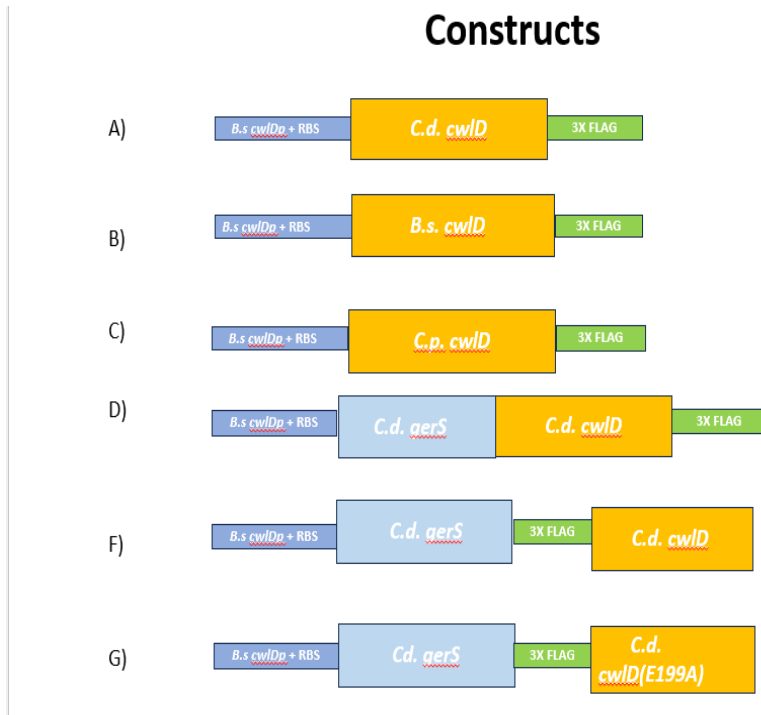


**Figure 3.2: Final Gibson Assembly Constructs**

Constructs A–G express several combinations of *cwID* and *gerS* genes under the control of the *B. subtilis cwID* promoter and RBS, coupled with a 3xFLAG tag for detection.

**Table 3.3: Summary of PCR products used for cloning of *cwlD* and *gerS* constructs.**

PCR template	Lane	Description	Primers Used (Table 2.1)	Expected Band (bp)
	1	Ladder	-	-
pDPV937	2	<i>B.s. cwlDp-RBS</i> for expressing <i>cwlD</i>	956 + 958	118
pDPV937	3	<i>B.s. cwlDp-RBS</i> for expressing <i>gerS</i>	956 + 957	126
pDPV1022	4	<i>C.d. cwlD-3XFLAG</i>	964 + 962	1047
pDPV1023	5	<i>B.s. cwlD-3Xflag</i>	1023 + 962	1051
pDPV1024	6	<i>C.p. cwlD-3xFLAG</i>	1064 + 962	1014
pDPV938	7	<i>C.d. gerS</i>	959 + 960	615
pDPV1022	8	<i>C.d. cwlD-3xFLAG</i>	961 + 962	1047
pDPV938	9	<i>C.d. cwlD</i>	1066 + 962	1024
pDPV939	10	<i>C.d. cwlD(E199A)</i>	1066 + 962	1024
pDPV937	11	<i>B.s. cwlDp-RBS</i> for expressing <i>B.s. cwlD</i>	956 + 1022	118
pDPV937	12	<i>B.s. cwlDp-RBS</i> for expressing <i>C.p. cwlD</i>	956 + 1063	118

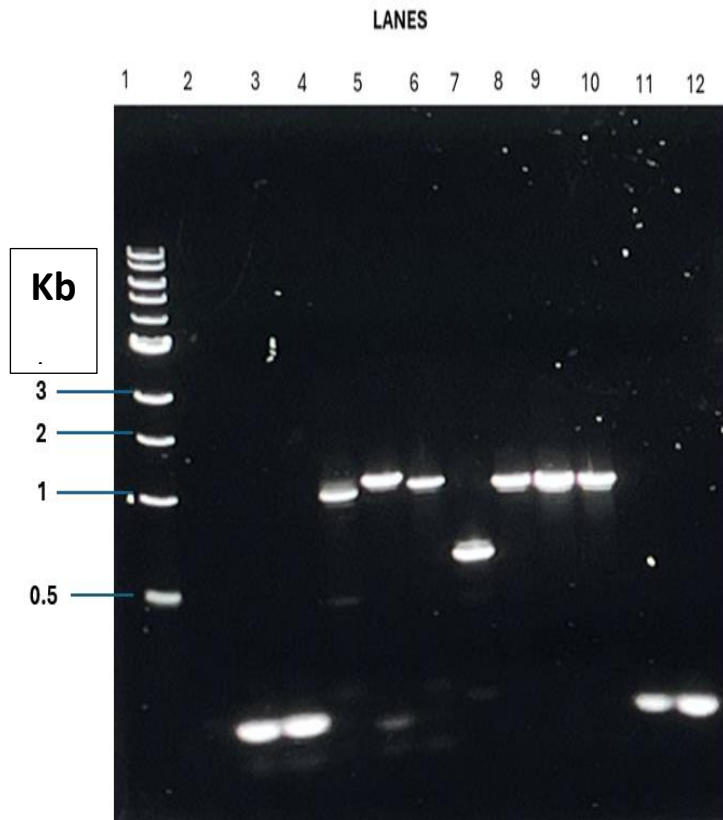


**Figure 3.3: Agarose gel electrophoresis of PCR-amplified *cwID* and *gerS* constructs.**

The representative gel image displays PCR results associated with diverse gene constructs utilized for cloning. The lanes comprise amplicons for *cwID* and *gerS*, encompassing RBS derived from *B. subtilis*, *cwID* from *B. subtilis*, *C. difficile*, and *C. perfringens*, and *gerS* from *C. difficile*, as well as 3xFLAG-tagged variants. Each band corresponds to the anticipated product dimensions, as specified in Table 3.3. A 1 kb DNA ladder was employed for size estimation.

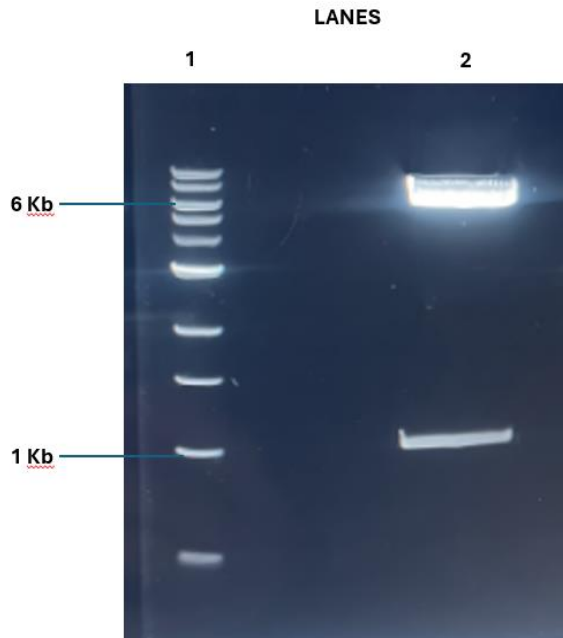


**Figure 3.4: Agarose gel displaying pBS1E plasmid linearization.**

Lane 1 shows the 1 kb DNA ladder. Lane 2 shows two fragments (~6 kb and ~1.1 kb) arising from XbaI and SpeI digestion. Two separate DNA fragments were found by agarose gel electrophoresis: a smaller ~1.1 kb band for the removed RFP gene and a large ~6 kb band corresponding to the plasmid backbone.

**Table 3.4: Description of the assembled plasmid constructions**

<b>Assembly</b>	<b>Description</b>	<b>Vector</b>	<b>PCR 1</b>	<b>PCR 2</b>	<b>PCR 3</b>
A	<i>C.d. CwID-3xFLAG</i>	pBS1E SpeI-XbaI	<i>B.s. cwIDp-RBS for expressing cwID</i>	<i>C.d. cwID-3Xflag</i>	
B	<i>B.s. CwID-3xFLAG</i>	pBS1E SpeI-XbaI	<i>B.s. cwIDp-RBS for expressing B.s. cwID</i>	<i>B.s. cwID-3xFLAG</i>	
C	<i>C.p. CwID-3xFLAG</i>	pBS1E SpeI-XbaI	<i>B.s. cwIDp-RBS for expressing C.p. cwID</i>	<i>C.p. cwID-3xFLAG</i>	
D	<i>C.d. GerS-CwID-3xFLAG</i>	pBS1E SpeI-XbaI	<i>B.s. cwIDp-RBS for expressing gerS</i>	<i>C.d. gerS</i>	<i>C.d. cwID-3Xflag</i>
F	<i>C.d. GerS-3xFLAG -CwID</i>	pBS1E SpeI-XbaI	<i>B.s. cwIDp-RBS for expressing gerS</i>	<i>C.d. gerS-3xFLAG</i>	<i>C.d. cwID</i>
G	<i>C.d. GerS-3xFLAG - CwID(E199A)</i>	pBS1E SpeI-XbaI	<i>B.s. cwIDp-RBS for expressing gerS</i>	<i>C.d. gerS-3xFLAG</i>	<i>C.d. cwID(E199A)</i>

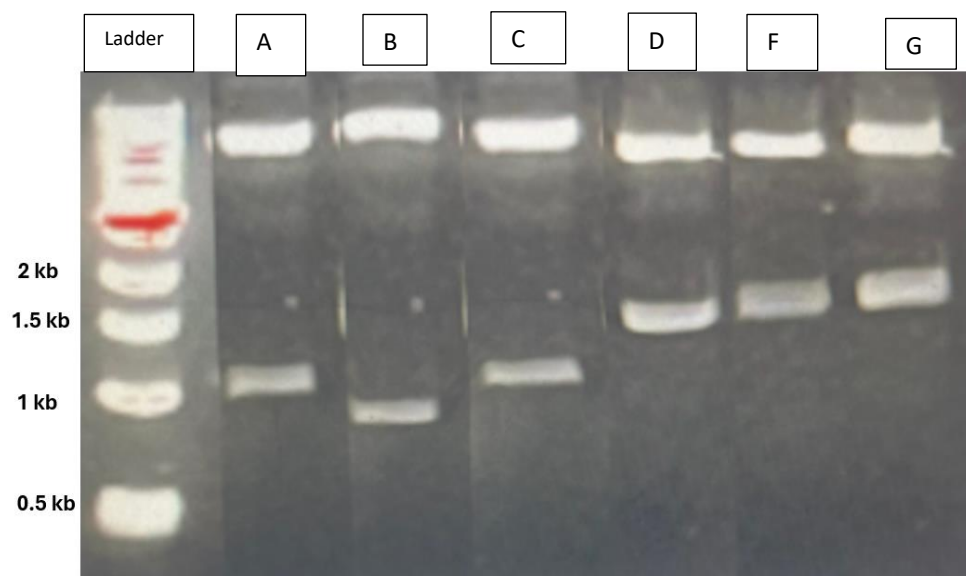


**Figure: 3.5: Agarose gel image of restriction digest results for assembled plasmids.**

All plasmids were validated via restriction enzyme digestion to confirm proper integration and insert size. Digested products were resolved on agarose gels and matched the expected fragment sizes (Table 3.5). The constructs yielded clean and precise digestion profiles. Constructions had successful absorption of Gibson-assembled plasmids transformed into *E. coli* VE3 cells. On selective LB + ampicillin agar plates for Assemblies A through G, white colonies revealed appropriate plasmid integration and RFP disturbance. Confirmation by Sequencing Sanger sequencing further validated the accuracy and orientation of all inserts except A. The other sequences matched expected templates with high fidelity, including the point mutation (E199A) in the catalytic site of CwID. No frameshifts or unintended mutations were observed. Assembly A, initially unsuccessful, was confirmed through re-assembly, transformation, and sequencing from VE3, but still failed to show a positive result. This confirms that the electroporation of the Gibson assembly product into the VE3 was successful.

**Table 3.5: Restriction digest analysis of Gibson-assembled plasmids.**

Assembly	Restriction Enzymes	Expected Bands (bp)	Result	<i>E. coli</i> strain in lab collection
A	EcoRI, SpeI	1116 bp, 6082 bp	Correct	-
B	EcoRI, PvuII	999 bp, 6196 bp	Correct	DPVE1064
C	EcoRI, SpeI	1083 bp, 6082 bp	Correct	DPVE1065
D	EcoRI, SpeI	1719 bp, 6082 bp	Correct	DPVE1066
F	EcoRI, SpeI	1719 bp, 6082 bp	Correct	DPVE1067
G	EcoRI, SpeI	1719 bp, 6082 bp	Correct	DPVE1068

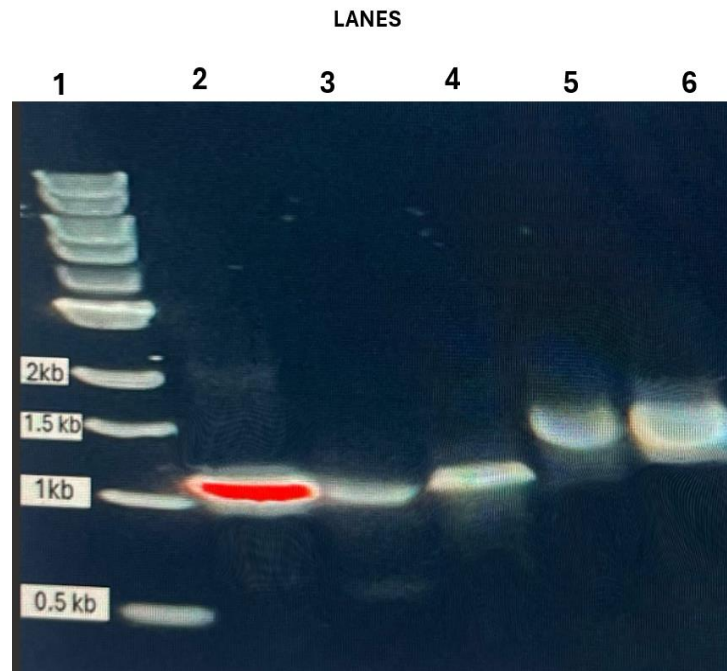


**Figure 3.6: Chromosomal integration of plasmid constructs into *B. subtilis* Acw1D.**

PCR using insertion-specific primers (Table 2.1) started using genomic DNA from transformed *B. subtilis* colonies. All lanes generated single amplicons of predicted size, therefore verifying appropriate recombination at the *amyE* locus.

**Table 3.6: Gel Electrophoresis Results**

Lane	Description	Expected Band (bp)	Result	<i>B. subtilis</i> strain in the lab collection
Lane 1	Ladder	-	-	
Lane 2 (B)	<i>B. subtilis</i> <i>CwlD</i> - <i>3xFLAG</i>	1169	Correct	DPVB1189
Lane 3 (C)	<i>C. perfringens</i> <i>CwlD</i> - <i>3xFLAG</i>	1192	Correct	DPVB1190
Lane 4 (D)	<i>C. difficile</i> <i>GerS</i> - <i>CwlD</i> - <i>3xFLAG</i>	1178	Correct	DPVB1191
Lane 5 (F)	<i>C. difficile</i> <i>GerS</i> - <i>3xFLAG</i> – <i>CwlD</i>	1837	Correct	DPVB1192
Lane 6 (G)	<i>C. difficile</i> <i>GerS</i> - <i>3xFLAG</i> – <i>CwlD</i> (E199A)	1837	Correct	DPVB1193

### 3.3. Growth, Sporulation, and Protein Detection using FLAG-Tagged

#### Constructs:

The beginning of sporogenesis ( $T_0$ ) was marked by Sporulation and morphological observation of FLAG-Tagged Constructs *Bacillus subtilis*  $\Delta cwlD$  strains reaching an  $OD_{600}$  of 3.0. Four hours later, or  $T_4$ , samples revealed mid-to-late sporogenesis phases. Phase-bright spores, swallowed forespores, and mother cell compartments compatible with continuous spore growth were identified by a microscopic study of  $T_4$  samples. These results verified that the strains moved through sporogenesis and produced enough biomass for the study of downstream protein expression.

FLAG-tagged protein expression in sporulating *B. subtilis* strains was assessed by western blotting (Figure 3.7 and Table 3.7). Lane 2 shows a distinct ~30 kDa band matching *B. subtilis* CwlD-3xFLAG. In lanes 3–6, which represent other FLAG-tagged constructions, no signal was seen. Imaging total proteins verified even loading in all lanes. Low expression, instability of the tagged proteins, or destruction during sporogenesis could all help to explain the absence of a clear signal in these constructions.

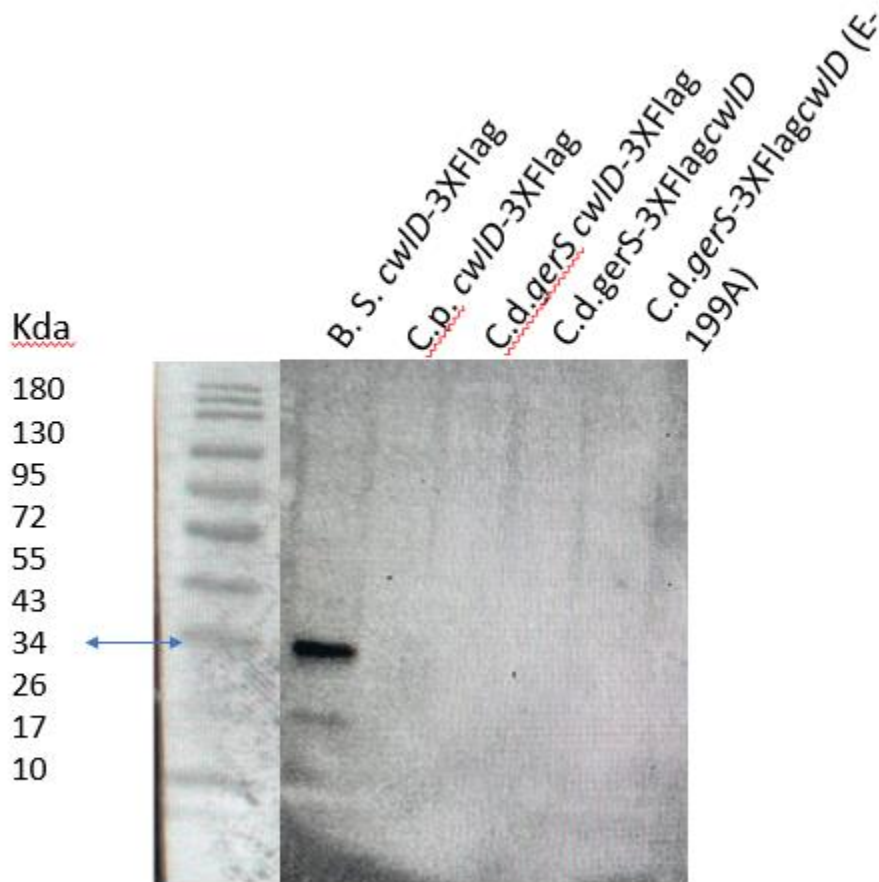


**Figure 3.7 Western Blot Detection of GerS Proteins and FLAG-Tagged CwID**

While no signal was seen for any of the FLAG-tagged constructs generated from *C. perfringens* or *C. difficile*, Western blot analysis demonstrated specific identification of the *B. subtilis* CwID-3xTAG protein (~30 kDa). Consistent loading across all lanes was confirmed by total protein stain-free imaging, therefore removing unequal protein input as a contributing cause for the poor results. Table 3.7 identifies the lanes, samples, and expected bands.

**Table 3.7: Western Blot Results**

<b>Lane</b>	<b>Description</b>	<b>Expected Band (kDa)</b>	<b>Result</b>
Lane 1	Ladder	-	-
Lane 2 Construct B (fig:3.2)	<i>B. subtilis</i> CwID-3xFLAG	30 kDa	Correct
Lane 3 Construct C (fig:3.2)	<i>C. perfringens</i> CwID-3xFLAG	28 kDa	Incorrect
Lane 4 Construct D (fig:3.2)	<i>C. difficile</i> GerS-CwID-3xFLAG	29.9 kDa	Incorrect
Lane 5 Construct F (fig:3.2)	<i>C. difficile</i> GerS-3xFLAG – CwID	25.96 kDa	Incorrect
Lane 6 Construct G (fig:3.2)	<i>C. difficile</i> GerS-3xFLAG – CwID(E199A)	29.96 kDa	incorrect

### 3.4. Germination efficiency of recombinant *B. subtilis* strains

To evaluate the efficacy of different CwID constructions in rectifying the germination deficiency in a *B. subtilis*  $\Delta cwID$  mutant, spore suspensions were standardized to OD<sub>600</sub> = 0.2, serially diluted, plated on LB agar, and colony-forming units (CFUs) were counted post-incubation.

Germination efficiency was quantified as CFU/OD<sub>600</sub>/ml. Wild-type spores demonstrated vigorous germination, yielding CFU/OD<sub>600</sub>/ml levels above 10<sup>10</sup>. Conversely, the  $\Delta cwID$  mutant exhibited a significant germination impairment, with CFU/OD<sub>600</sub>/ml counts decreased by over five orders of magnitude. The expression of *B. subtilis* *CwID-3* × *FLAG* reinstated germination efficiency 1000-fold, but still 100-fold less than wild-type, demonstrating partial complementation. Nevertheless, constructions expressing CwID from *C. perfringens* or *C. difficile*, whether independently or in conjunction with GerS, did not completely restore germination. These strains produced significantly reduced CFU counts, indicating that heterologous CwID proteins are ineffective in the *B. subtilis* environment. Significantly, the co-expression of *C. difficile* GerS–CwID (E199A) led to a partial recovery, with CFUs roughly 100-fold lower than the wild type, suggesting limited yet incomplete complementation.

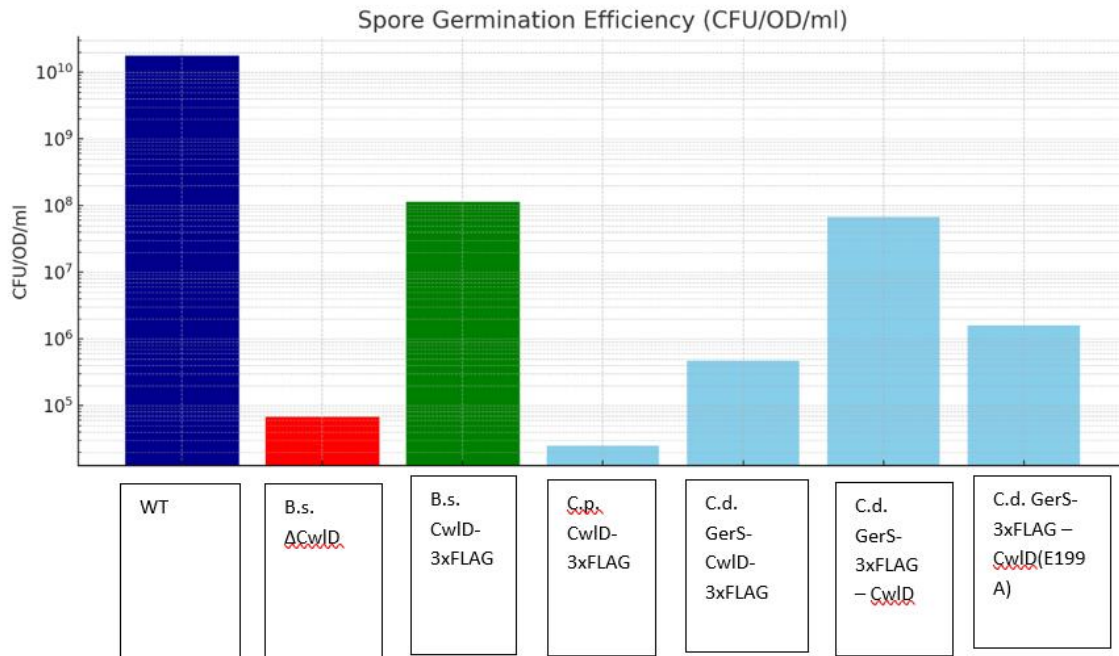


**Figure 3.8: Spore germination efficiency of  $\Delta cwID$  strains expressing various CwID constructs.**

This is data derived from a single assay. Germination efficiency was quantified by measuring CFU/OD<sub>600</sub>/ml and plating of purified spores. Wild-type spores produced extremely high colony counts, while the  $\Delta cwID$  mutant showed a severe germination defect. Expression of *B. subtilis* CwID-3×FLAG restored germination to near wild-type levels. Complementation with *C. perfringens* or *C. difficile* CwID constructs—including those co-expressed with GerS—failed to fully restore germination. Notably, strain F (*C.d. GerS-CwID*) displayed partial recovery (~100-fold lower than WT), indicating possible leaky germination but incomplete complementation.

### 3.5. Spore cortex structure of recombinant *B. subtilis* strains:

Muramic- $\delta$ -lactam (MAL), a peptidoglycan alteration specific to the cortex, served as an indicator of effective CwID-dependent remodeling. The wild-type strain exhibited prominent MAL-associated peaks, whereas the  $\Delta cwID$  mutant was devoid of these characteristics (Fig. 3.9). The expression of *B. subtilis* CwID-3 $\times$ FLAG reinstated MAL production, signifying functional complementation. No MAL peaks were seen in strains expressing *C. perfringens* CwID, *C. difficile* GerS-CwID (with or without independent GerS expression), or the inactive CwID(E199A), indicating an inability to restore normal cortical structure.

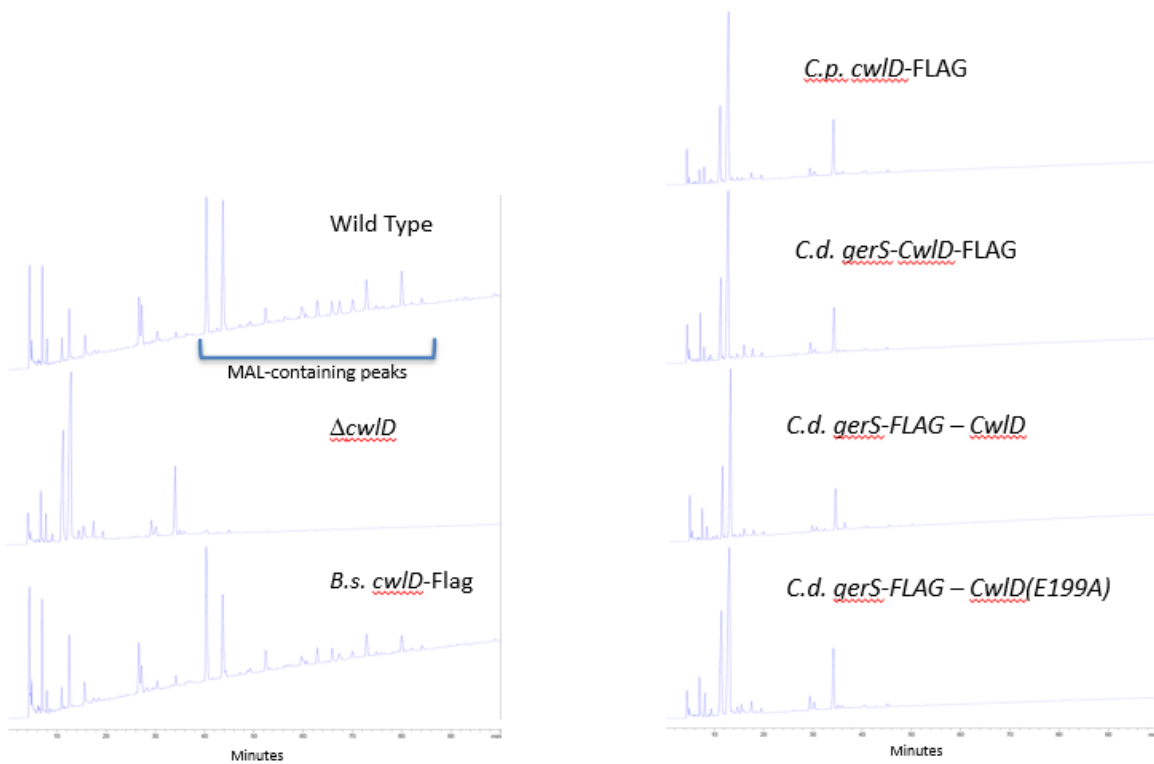


**Figure 3.9: HPLC profiles of muuropeptides generated from the cortex of recombinant *B. subtilis* strains.**

Muropeptides, including muramic- $\delta$ -lactam (MAL), indicative of cortex-specific remodeling, were identified in wild-type spores but not in the  $\Delta cwID$  mutant. Restoring MAL peaks following complementation with *B. subtilis* CwID-3 $\times$ FLAG indicates functional activity. No MAL was seen in strains expressing *C. perfringens* CwID, *C. difficile* GerS-CwID (regardless of the presence of distinct GerS), or the inactive CwID(E199A) mutant, indicating an inability to facilitate appropriate cortical remodeling.

## CHAPTER 4: DISCUSSION

This work aimed to ascertain whether expression of FLAG-tagged CwID and GerS proteins from *C. difficile* in a *B. subtilis*  $\Delta cwID$  background could be obtained and if they would complement CwID activity. These proteins, which are known to be necessary for cortical remodeling and spore germination in *C. difficile*, were expected to be functionally produced and maybe restore germination deficits in the  $\Delta cwID$  mutant. Western blot investigation utilizing anti-FLAG antibodies failed to find any expression from the heterologous constructs, even though all genetic constructs were correctly assembled, sequenced, and integrated into the *B. subtilis* chromosome. By contrast, the robust expression of the *B. subtilis* *CwID-3xFLAG* control indicated the system was operational. So, why were the proteins not expressed? There are a few likely answers. One of the most likely is that the heterologous proteins were unstable or misfolded in *B. subtilis*, hence broken down by the host's quality control systems. To be effective in *C. difficile*, CwID needs interaction with a lipoprotein termed GerS. Important for CwID amidase action; GerS enables CwID to fold properly and bind zinc. Without this partner, or should GerS itself fail to operate, CwID might not fold well and is most likely targeted for degradation. Now, the next question arises that why might GerS fail in *B. subtilis*? Being a lipoprotein, GerS is anchored to the membrane using lipidation. Near the start of the protein, this action takes place at a particular amino acid, a cysteine. Lipidation cannot occur without the host identifying a signal sequence at the N-terminus of a protein and modifying it with particular enzymes (42). Should *B. subtilis* fail to identify the *C. difficile* GerS signal, its processing could be compromised. GerS would remain unaltered, remain in an incorrect location, or misfold and might get degraded. This would keep it from enabling CwID to localize or stabilize appropriately. Another potential reason for the failure of protein expression could be failure at a transcriptional

level. We constructed an artificial operon to express GerS and CwID in *B. subtilis*. To guarantee they are transcribed together as one mRNA and ideally translated in equal amounts, we put both genes under a single promoter and ribosome binding site. In our experiment, this did not produce any observable protein expression in *B. subtilis*. Given the intact and accurate insertion of the DNA sequence, this suggests issues not in the DNA but rather in RNA stability, protein translation, or post-translational modifications.

Another potential explanation for translation obstacles could be codon bias. Certain codons are preferred by each organism for the encoding of identical amino acids. The translation efficiency may decrease as a result of ribosomal pausing or stalling when a heterologous gene contains uncommon codons that are not frequently used in the host (46). It is important to note that *B. subtilis* has a GC content of approximately 43.5–43.8% (47), while *C. perfringens* and *C. difficile* have significantly reduced GC contents (about 28.6% and 28–30% respectively)(41, 48, 49). These differences may lead to codon usage mismatches that might impede the efficient translation of *C. difficile* or *C. perfringens* genes in *B. subtilis*, thereby diminishing protein yield or stability.

Furthermore, this work detected a 3xFLAG tag using anti-FLAG antibodies. Small, often non-disruptive, FLAG tags are valuable since they can be utilized across several constructions (41). However, employed anti-CwID antibodies, specific to the natural protein. Here for flexibility—to evaluate several constructions from various species under the same detection method—the move to FLAG was made. Still, FLAG detection relies on whether the tag is exposed and not cleaved off. The antibody might not find the FLAG tag if the protein folds in such a way that hides it or if it is rapidly destroyed. This helps to explain why Kohler saw *C. difficile* CwID and GerS expression when we did not.

Though it is unfortunate, the lack of obvious expression is instructive. Our results complement earlier ideas stressing the complex and strictly controlled character of spore protein interactions, particularly across different species. Even highly conserved genes need a completely functional and compatible translation system for effective expression; so, functional failure can result from disturbance of the system(50). This underscores the fact that protein expression deficiencies are not always the result of genetic issues; rather, they may be the consequence of deficiencies in the cellular machinery necessary for translation. The stage at which expression is inhibited could be narrowed by measuring mRNA transcript levels using RT-qPCR. The issue is likely to arise at the post-translational level if transcripts are detected but corresponding proteins are absent. In contrast, the absence of transcripts may suggest issues with the target site's genomic integration or promoter activity.

Future constructions should meet *B. subtilis* preferences using codon optimization. Fusion to Green fluorescent protein (GFP) could provide improved tracking of expression and localization. Additionally, co-expression of known *C. difficile* lipidation or folding proteins, such as chaperones or membrane-associated enzymes, may improve the stability, processing, or proper localization of GerS and CwID in a heterologous host. On the other hand, *in vitro* protein expression employing *E. coli* could remove these obstacles and enable biochemical characterization. Although FLAG-tagged CwID and GerS were not found in *B. subtilis*, this offers an important new perspective on the restrictions associated with heterologous protein expression between species. It underlines that without the appropriate biological setting; even well-designed genetic constructions could fail. These results underline the need to consider host-specific translation, folding, and localization needs while working with complicated, multi-component protein systems.

## CHAPTER 5: CONCLUSION

This work aimed to examine the capacity of FLAG-tagged *C. difficile* CwID and GerS proteins in a *B. subtilis*  $\Delta cwID$  background to complement CwID function. Western blotting revealed no *C. difficile* protein expression despite successful construct assembly and chromosomal integration, even though a *B. subtilis* cwID-3xFLAG control expressed robustly. These results imply that either signal recognition, lipidation, codon use, or post-translational quality control caused incompatibility in protein stability, folding, or translation, impairing cross-species expression at that level. The findings confirm that CwID and GerS proteins in *C. difficile* may require particular cellular components for stability, which are absent or incompatible in *B. subtilis*. These results draw attention to the extremely specific character of spore cortical remodeling machinery and show the difficulties of producing spore-associated proteins across species.

## Reference

1. B. K. Sandhu, S. M. McBride, *Clostridioides difficile*. *Trends in microbiology* 26, 1049-1050 (2018).
2. J. K. Cheng, M. Unnikrishnan, *Clostridioides difficile* infection: traversing host–pathogen interactions in the gut. *Microbiology* 169, 001306 (2023).
3. R. McConnie, A. Kastl, *Clostridium difficile*, colitis, and colonoscopy: pediatric perspective. *Current gastroenterology reports* 19, 1-5 (2017).
4. E. Finn, F. L. Andersson, M. Madin-Warburton, Burden of *Clostridioides difficile* infection (CDI)-a systematic review of the epidemiology of primary and recurrent CDI. *BMC infectious diseases* 21, 456 (2021).
5. M. Goudarzi, S. S. Seyedjavadi, H. Goudarzi, E. Mehdizadeh Aghdam, S. Nazeri, *Clostridium difficile* infection: epidemiology, pathogenesis, risk factors, and therapeutic options. *Scientifica* 2014, 916826 (2014).
6. J. S. Martin, T. M. Monaghan, M. H. Wilcox, *Clostridium difficile* infection: epidemiology, diagnosis and understanding transmission. *Nature reviews Gastroenterology & hepatology* 13, 206-216 (2016).
7. L. C. McDonald *et al.*, Clinical practice guidelines for *Clostridium difficile* infection in adults and children: 2017 update by the Infectious Diseases Society of America (IDSA) and Society for Healthcare Epidemiology of America (SHEA). *Clinical infectious diseases* 66, e1-e48 (2018).
8. D. Paredes-Sabja, A. Shen, J. A. Sorg, *Clostridium difficile* spore biology: sporulation, germination, and spore structural proteins. *Trends in microbiology* 22, 406-416 (2014).
9. D. M. Maynard (2024) L-arabinose Induced Overexpression for Crystallographic Analysis of the SpoIIE Protein from *Clostridioides difficile*. (University of Arkansas).

10. M. A. Al-Hinai, S. W. Jones, E. T. Papoutsakis, The *Clostridium* sporulation programs: diversity and preservation of endospore differentiation. *Microbiology and Molecular Biology Reviews* 79, 19-37 (2015).
11. J. Errington, Regulation of endospore formation in *Bacillus subtilis*. *Nature Reviews Microbiology* 1, 117-126 (2003).
12. D. Zhu, J. A. Sorg, X. Sun, *Clostridioides difficile* biology: sporulation, germination, and corresponding therapies for *C. difficile* infection. *Frontiers in cellular and infection microbiology* 8, 29 (2018).
13. J. Czepiel *et al.*, *Clostridium difficile* infection. *European journal of clinical microbiology & infectious diseases* 38, 1211-1221 (2019).
14. S. Ghosh, P. Setlow, Isolation and characterization of superdormant spores of *Bacillus* species. *Journal of Bacteriology* 191, 1787-1797 (2009).
15. A. E. Cowan *et al.*, Lipids in the inner membrane of dormant spores of *Bacillus* species are largely immobile. *Proceedings of the National Academy of Sciences* 101, 7733-7738 (2004).
16. D. L. Popham, J. Helin, C. E. Costello, P. Setlow, Muramic lactam in peptidoglycan of *Bacillus subtilis* spores is required for spore outgrowth but not for spore dehydration or heat resistance. *Proceedings of the National Academy of Sciences* 93, 15405-15410 (1996).
17. H. Coullon *et al.*, N-Deacetylases required for muramic- $\delta$ -lactam production are involved in *Clostridium difficile* sporulation, germination, and heat resistance. *Journal of Biological Chemistry* 293, 18040-18054 (2018).
18. L. Liang *et al.*, Evaluation of fungal spore characteristics in Beijing, China, based on molecular tracer measurements. *Environmental Research Letters* 8, 014005 (2013).
19. S. Makino, R. Moriyama, Hydrolysis of cortex peptidoglycan during bacterial spore germination. *Medical Science Monitor* 8, RA119-RA127 (2002).
20. A. Driks, P. Setlow, Morphogenesis and properties of the bacterial spore. *Prokaryotic Development*, 191-218 (1999).

21. P. Setlow, Germination of Spores of *Bacillus* Species: What We Know and Do Not Know. *Journal of Bacteriology* 196, 1297-1305 (2014).
22. J. A. Sorg, A. L. Sonenshein, Bile salts and glycine as cogerminants for *Clostridium difficile* spores. *Journal of bacteriology* 190, 2505-2512 (2008).
23. W. Vollmer, B. Joris, P. Charlier, S. Foster, Bacterial peptidoglycan (murein) hydrolases. *FEMS microbiology reviews* 32, 259-286 (2008).
24. D. L. Popham, C. B. Bernhards, Spore peptidoglycan. *The bacterial spore: from molecules to systems*, 157-177 (2016).
25. A. Warth, J. Strominger, Structure of the peptidoglycan of bacterial spores: occurrence of the lactam of muramic acid. *Proceedings of the National Academy of Sciences* 64, 528-535 (1969).
26. W. Li, S. Mednick, P. Setlow, Y.-Q. Li, Modeling heterogeneity, commitment, and memory of bacterial spore germination. *mBio*, e00596-00525 (2025).
27. Y. Imae, J. L. Strominger, Cortex content of asporogenous mutants of *Bacillus subtilis*. *Journal of Bacteriology* 126, 914-918 (1976).
28. B. Setlow, E. Melly, P. Setlow, Properties of Spores of *Bacillus subtilis* Blocked at an Intermediate Stage in Spore Germination. *Journal of Bacteriology* 183, 4894-4899 (2001).
29. K. W. Bollinger *et al.*, Identification of a family of peptidoglycan transpeptidases reveals that *Clostridioides difficile* requires noncanonical cross-links for viability. *Proceedings of the National Academy of Sciences* 121, e2408540121 (2024).
30. A. Atrih, P. Zöllner, G. Allmaier, S. J. Foster, Structural analysis of *Bacillus subtilis* 168 endospore peptidoglycan and its role during differentiation. *Journal of Bacteriology* 178, 6173-6183 (1996).
31. T. J. Kochan *et al.*, Updates to *Clostridium difficile* Spore Germination. *Journal of Bacteriology* 200, 10.1128/jb.00218-00218 (2018).
32. D. Bhattacharjee, K. N. McAllister, J. A. Sorg, Germinants and Their Receptors in *Clostridia*. *Journal of Bacteriology* 198, 2767-2775 (2016).

33. A. Shen, A. N. Edwards, M. R. Sarker, D. Paredes-Sabja, Sporulation and Germination in *Clostridial* Pathogens. *Microbiology Spectrum* 7, 10.1128/microbiolspec.gpp1123-0017-2018 (2019).
34. D. E. Voth, J. D. Ballard, *Clostridium difficile* Toxins: Mechanism of Action and Role in Disease. *Clinical Microbiology Reviews* 18, 247-263 (2005).
35. S. E.-M. A. Hall\*, Rho GTPases in cell biology. *NATURE* VOL 420 (R 2002).
36. Shannon L. Kordus 1, 4, Audrey K. Thomas<sup>1,2,4</sup> and D. Borden Lacy, *Clostridioides difficile* toxins: mechanisms of action and antitoxin therapeutics. *Nature Reviews Microbiology* volume 20 (2022).
37. X. L. Zheng-Ming Wang, Ross R. Cocklin, Minhui Wang, Mu Wang, Koichi Fukase, S. K. Seiichi Inamura, Dipika Gupta, and Roman Dziarski, Human Peptidoglycan Recognition Protein-L Is an N-Acetylmuramoyl-L-alanine Amidase. *Journal of Biological Chemistry* Volume 278 (2023).
38. B. Salamaga *et al.*, Demonstration of the role of cell wall homeostasis in *Staphylococcus aureus* growth and the action of bactericidal antibiotics. *Proceedings of the National Academy of Sciences* 118, e2106022118 (2021).
39. D. L. Popham, C. B. Bernhards, "Spore Peptidoglycan" in *The Bacterial Spore*. (2016), pp. 157-177.
40. J. O. Fimlaid KA, Donnelly ML, Siegrist MS, Shen A Regulation of *Clostridium difficile* Spore Formation by the SpoIIQ and SpoIIIAProteins. *PLOS Genetics* (2015).
41. B. J. Kohler (2023) Investigating the enzyme activity of a *Clostridioides difficile* amidase complex. in *Biological Sciences* (Virginia Tech, Blacksburg, Va).
42. B. E. E. Carolina Alves Feliciano<sup>1</sup>, O. R. D. b. 2, Sylvie Doublet<sup>2</sup>, Aimee Shen, A lipoprotein allosterically activates the CwID amidase during *Clostridioides difficile* spore formation. *PLOS GENETICS* (2021).

43. M. H. Touchette *et al.*, Identification of a Novel Regulator of *Clostridioides difficile* Cortex Formation. *mSphere* 6, 10.1128/msphere.00211-00221 (2021).
44. M. E. Gilmore, D. Bandyopadhyay, A. M. Dean, S. D. Linnstaedt, D. L. Popham, Production of Muramic- $\delta$ -Lactam in *Bacillus subtilis* Spore Peptidoglycan. *Journal of Bacteriology* 186, 80-89 (2004).
45. B. Barat (2020) Characterization of proteins involved in *Bacillus subtilis* spore formation and germination. in *Biological Sciences* (VirginiaTech, Blacksburg, Virginia).
46. H. Gingold, Y. Pilpel, Determinants of translation efficiency and accuracy. *Molecular Systems Biology* 7, 481 (2011).
47. F. Kunstl *et al.*, The complete genome sequence of the Gram-positive bacterium *Bacillus subtilis*. *Nature* 390 (1997).
48. T. Shimizu *et al.*, Complete genome sequence of *Clostridium perfringens*, an anaerobic flesh-eater. *Proceedings of the National Academy of Sciences* 99, 996-1001 (2002).
49. K. V. Cundy *et al.*, Comparison of traditional gas chromatography (GC), headspace GC, and the microbial identification library GC system for the identification of *Clostridium difficile*. *Journal of Clinical Microbiology* 29, 260-263 (1991).
50. E. V. Koonin, Y. I. Wolf, Genomics of bacteria and archaea: the emerging dynamic view of the prokaryotic world. *Nucleic Acids Research* 36, 6688-6719 (2008).